Journal of Integrative Agriculture 2026, 25(8): 3194–3207

Available online at ScienceDirect

Journal of Integrative Agriculture



RESEARCH ARTICLE

Micro-sprinkler irrigation induces synergistic source–sink regulation: A promising strategy for boosting wheat grain weight in the Huaibei Plain, China

Siqi Wang[1], Mengyu Sun[1], Kaiyi Xing[1], Xin Cheng[1], Le Wang[1], Limeng Zhang[1], Chunsheng Yao[1], Yinghua Zhang[2], Zhimin Wang[2], He Song[1#], Jinpeng Li[1#]

[1] *College of Agronomy, Anhui Agricultural University, Hefei 230036, China*
[2] *College of Agronomy and Biotechnology, China Agricultural University, Beijing 100193, China*

Highlights

- Micro-sprinkler irrigation (MI) increased the number of endosperm cells in grain by regulating hormone metabolism.
- MI enhanced sucrose synthesis capacity after anthesis, thereby promoting grain filling.
- MI improved the 1,000-grain weight and grain yield when it obtained the highest spike number and grain number per spike at maturity.

Abstract

Enhancing wheat grain weight is a crucial strategy for improving yields in the Huaibei Plain (HP), China. However, the impacts and regulatory mechanisms of different irrigation regimes on wheat grain formation in the HP remained poorly understood. Therefore, a two-year field experiment was conducted to explore three treatments on wheat's source–sink relationship and grain formation: rain-fed (RI, no irrigation, 202.5 kg ha^{-1} N applied at sowing), conventional flood irrigation (CI, 60 mm irrigation at jointing stage, 112.5 kg ha^{-1} N at sowing+90 kg ha^{-1} N with irrigation), and micro-sprinkler irrigation (MI, irrigation based on 0–40 cm soil layer water deficit at jointing, booting and anthesis stages, 112.5 kg ha^{-1} N at sowing+30 kg ha^{-1} N at each irrigation). The results indicated that, compared with RI and CI, MI significantly increased chlorophyll content and enhanced sucrose phosphate synthase (SPS) activity in the flag leaf at 4 days after anthesis (DAA 4), and these parameters in CI were higher than those in RI. The sucrose and soluble sugar content in the grain of MI were the highest at DAA 4. Additionally, at DAA 4, compared with RI, both CI and MI significantly elevated the content of indole propionic acid+zeatin nucleoside (IPA+ZR) and gibberellin (GA) in grain, while reducing the content of auxin (IAA) and abscisic acid (ABA). And the highest number of endosperm cells was observed in MI. At the grain-filling stage, MI exhibited the slowest chlorophyll degradation rate and the highest activities of ribulose-1,5-bisphosphate carboxylase/oxygenase (Rubisco) and SPS in the flag leaf, resulting in more sugar accumulation in the leaf and grain. Moreover, MI showed the highest IAA and lowest ABA levels in grain and maintained the highest starch synthase activity during the filling stage, thereby promoting starch accumulation. Compared to CI and RI, MI significantly increased 1,000-grain weight by 4.99–5.55% and 7.33–11.51%, and grain yield by 4.99–11.60% and 15.60–39.14% over the two years, respectively. Overall, micro-sprinkler irrigation can optimize the water and nitrogen supply for wheat, effectively enhancing the source capacity in the early stage and the sink capacity in the late stage of grain development, thereby increasing grain weight and achieving high yield in the HP.

Keywords: irrigation regimes, source–sink relationship, grain formation, starch accumulation, grain yield

1. Introduction

Wheat, as one of the most important food crops globally, plays a pivotal role in ensuring global food security. With the global population continuing to grow, increasing wheat yield has emerged as a critical task to address food security challenges (Yang *et al.* 2013). Grain weight, number of

Received 15 September 2025; Received in revised form 8 December 2025; Accepted 22 December 2025; Available online 16 January 2026
[#]Correspondence Jinpeng Li, E-mail: jinpeng0103@126.com; He Song, E-mail: songhesonghe@foxmail.com

© 2026 CAAS. Publishing services by Elsevier B.V. on behalf of KeAi Communications Co. Ltd. This is an open access article under the CC BY-NC-ND license (http://creativecommons.org/licenses/by-nc-nd/4.0/). Peer review under responsibility of Editorial Board of *Journal of Integrative Agriculture*.
doi: 10.1016/j.jia.2026.01.024

grains per spike, and number of spikes per unit area are key components of wheat yield. Grain weight, as one of the yield components, is the combined result of grain-filling duration, filling rate, and endosperm cell proliferation (Xie *et al.* 2015; Hisse *et al.* 2019). Endosperm cell proliferation in the early stage of grain development determines the final grain volume and cell number, and expanding the sink capacity while promoting subsequent grain filling is an important basis for achieving high grain weight. Photosynthate accumulation during the grain-filling period is critical for determining grain dry matter weight, and its rate is closely related to the photosynthetic capacity of leaves (Alonso *et al.* 2018). During grain development, various factors, including genetic characteristics (Yu *et al.* 2022), climate change (Thapa *et al.* 2018), and water and fertilizer supply, influence grain weight (Yang *et al.* 2006; Yan *et al.* 2019). The Huaibei Plain (HP), a major wheat-producing region in China, faces a challenge: insufficient rainfall during the wheat-growing season fails to meet the crop's water demand during its critical growth periods, thereby hindering high-yield production (Gou *et al.* 2020). Moreover, the predominant lime concretion black soil in this region, which has clay characteristics and poor structure, tends to crack as soil water drops, exacerbating evaporation and causing water deficiency that impairs the vitality of wheat leaves or roots during grain filling, ultimately restricting assimilate accumulation in grain (Xu *et al.* 2006; Li J P *et al.* 2025). Therefore, appropriate irrigation management is a crucial measure to improve wheat grain weight and yield in the HP.

Wheat grain formation involves complex processes of photosynthate synthesis, absorption, transport, and accumulation. Source tissues provide essential nutrients for grain development, while sink tissues store and mobilize these resources (Abdelrahman *et al.* 2020; Xia *et al.* 2020). Some research indicates that grain weight is predominantly sink-limited (Serrago *et al.* 2013; Ahmed *et al.* 2024; Zhang *et al.* 2024), whereas others suggest it is significantly source-limited (Maydup *et al.* 2010). In fact, modern wheat genotypes are co-limited by both source and sink capacities rather than purely sink-limited, with winter wheat grain yield resulting from the synergistic interaction between source activity and sink strength (Lv *et al.* 2020). However, the relative importance of source and sink in grain formation remains controversial, largely due to variations in winter wheat varieties and growing environments across regions (Fang *et al.* 2022). The flag leaf, a crucial photosynthetic organ, plays a vital role in source establishment during grain development by generating and providing sufficient photosynthates for grain growth. Drought conditions have been shown to accelerate flag leaf chlorophyll degradation, leading to premature senescence, reduced photosynthate production, and ultimately decreased grain yield (Furbank *et al.* 2020; Wang *et al.* 2020). Conversely, optimal soil water for wheat after anthesis enhances flag leaf photosynthetic efficiency, promoting the synthesis of sugars and starch and thereby increasing source strength (Li *et al.* 2019). During grain filling, grains functioning as sink tissues begin utilizing and storing substances such as sugars and starch to facilitate grain growth. Adequate carbohydrates in grain enhance starch synthesis and transport, thereby increasing starch content and promoting grain formation through nutrient accumulation (Fan *et al.* 2024). At this stage, sink activity is a critical factor limiting grain weight, and the flag leaf's photosynthetic capacity for grain filling is likewise significant. Research has demonstrated that drought stress reduces grain sucrose synthesis and inhibits starch synthase activity, leading to decreased starch accumulation and reduced grain weight (Sehgal *et al.* 2018; Ru *et al.* 2024). By contrast, optimal soil water and nitrogen conditions coordinate post-anthesis nitrogen metabolism to enhance grain yield (Yao *et al.* 2024). For example, applying micro-sprinkler integrated water and fertilizer technology significantly enhances leaf nitrogen metabolism capacity during grain filling by ensuring late-stage nitrogen supply, thereby promoting protein accumulation in grain and increasing grain weight (Yao *et al.* 2023). Thus, rational water and N-fertilizer management strategies may be key to coordinating the source–sink relationship and improving grain weight.

Plant hormones, a class of trace organic substances synthesized by plant cells under induction, play a vital role in the grain-filling process. Endosperm cell proliferation determines the formation and size of the grain sink during the early stage of grain filling, and endogenous hormones in the grain directly influence assimilate supply and endosperm cell division, thereby regulating sink activity (Ma *et al.* 2023). In the early stage of wheat grain development, cytokinins (CTK) significantly promote endosperm cell division (Wang *et al.* 2015; Liu *et al.* 2016). Zeatin riboside (ZR) increases substantially during grain development and the peak period of cell division (Morris *et al.* 1993). Auxin (IAA) is also involved in regulating endosperm cell division during grain development, and high IAA concentrations can promote CTK accumulation in grain. Furthermore, grain gibberellin acid (GA) correlates with the grain-filling rate during the early filling stage, while abscisic acid (ABA) regulates grain dormancy and germination, affecting grain growth and development (Yang and Zhang 2006; Wang *et al.* 2015). Previous research indicates that soil water deficit can alter the synthesis, allocation, and transport of endogenous hormones, leading to changes in the dynamic balance (Peleg *et al.* 2011). When plants experience drought stress, the levels of indole-3-acetic acid (IAA), GA, and CTK decrease, whereas the level of ABA increases, thereby regulating physiological and biochemical processes that help plants adapt to drought (Farooq *et al.* 2009; Che *et al.* 2025). However, optimal irrigation delays flag leaf senescence and increases wheat yield by regulating endogenous hormones (Che *et al.* 2025). Consequently, coordinating the effects of different hormones and regulating hormone metabolism balance to promote grain development and formation is crucial for improving grain weight.

Appropriate water and fertilizer management is essential for crop growth and development (Li *et al.* 2019; Hao *et al.* 2024). Specifically, providing supplementary irrigation and topdressing at wheat's critical growth stages is crucial to improving grain yield. However, conventional flood irrigation not only easily causes water waste but also leads to soil compaction, which is unfavorable for the wheat root growing to the deep soil profile, reducing grain yield and water use

efficiency (Li J P *et al.* 2025; Li Z W *et al.* 2025). Meanwhile, one-time nitrogen topdressing at the jointing stage may not only increase ineffective tillers but also lead to nitrogen volatilization and leaching, lowering N-fertilizer use efficiency (Wang 2017; Li *et al.* 2018). Additionally, it exacerbates greenhouse gas emissions and pollutes the environment (Zhang *et al.* 2021). In recent years, micro-sprinkler irrigation technology has been gradually applied to wheat production. By adjusting water supply and delaying N-fertilizer application, it delays post-anthesis leaf senescence, maintains high photosynthetic capacity during grain filling, and achieves high yields while saving water and fertilizer, thus improving nitrogen and water use efficiency (Li *et al.* 2018; Zhai *et al.* 2021). Studies have shown that micro-sprinkler and deficit irrigation at the key growth stages significantly enhance wheat photosynthetic efficiency, maintain the photosynthetic capacity of the flag leaf during grain filling, effectively alleviate the impact of water stress on crops, promote grain filling, and increase grain weight and yield (Feng *et al.* 2017; Li *et al.* 2021; Bao *et al.* 2024). Previous research has also reported that during the jointing-to-anthesis stages of wheat, maintaining soil water content in the 0–40 cm soil profile at 70–85% of field capacity through supplementary irrigation is conducive to increasing grain yield (Lu *et al.* 2019). However, research on the impact of micro-sprinkler irrigation on wheat yield formation in the HP region remains limited, and the physiological mechanisms underlying the wheat source–sink relationship and post-anthesis grain formation under micro-sprinkler irrigation remain unclear.

In summary, this study hypothesizes that micro-sprinkler irrigation technology can optimize the source–sink relationship in wheat grains, regulate changes in endogenous hormones within grain, enhance source supply during the early grain-filling stage and sink activity in the late stage, delay leaf senescence, and promote grain filling, thereby ultimately increasing grain weight. The objectives of this study are to (1) analyze the effects of different water regimes on wheat grain formation and source–sink characteristics; (2) validate the hypothesis that micro-sprinkler irrigation can enhance wheat grain weight and elucidate the physiological mechanisms underlying its optimization of source–sink performance; and (3) establish a wheat management model suitable for the HP, providing a theoretical basis for increasing grain production under water-saving irrigation.

2. Materials and methods

2.1. Experimental site

The experiment was conducted from 2022 to 2024 at the Agricultural Scientific Institute (Mengcheng County, Bozhou City, Anhui Province, China; 33°9′44′′N, 116°32′56′′E). The experimental area is located in the Huaibei Plain (HP), the southernmost part of the Huang-Huai-Hai Plain. The local soil type is lime concretion black soil. Before the experiment, the contents of soil organic matter, total nitrogen, available phosphorus (P_2O_5), and available potassium (K_2O) contents in the 0–20 cm soil layer were 11.4 g kg^{-1}, 111.5 mg kg^{-1}, 61.7 mg kg^{-1}, and 188.9 mg kg^{-1}, respectively. The total rainfall and average annual temperature during the 2022–2023 and 2023–2024 wheat seasons were 359.00 mm and 11.51°C, and 370.10 mm and 11.21°C, respectively. The daily precipitation and air temperature variation during the two wheat growing seasons were shown in Fig. 1.

2.2. Experimental design

The experiment used Annong 0711 (AN0711), a semi-winter wheat variety widely cultivated in the HP, as test material. Three treatments were set up: rain-fed (RI, no irrigation), conventional flood irrigation (CI, 60 mm irrigation at the jointing stage), and micro-sprinkler irrigation (MI). MI was implemented using a micro-sprinkler hose at a flow rate of 6.0 m^3 h^{-1}, ensuring that the 0–40 cm soil layer was maintained at an appropriate field capacity (FC) during the jointing, booting, and anthesis stages. The wheat jointing (Z31), booting (Z45), and anthesis (Z61) stages were defined according to Zadoks scale (Zadoks *et al.* 1974). And taking into account the weather forecast and rainfall event from the jointing (Z31) to the anthesis (Z61) stage between the two years, with less rainfall in the 1st year and relatively more rainfall in the 2nd year, we set the soil water measurement target at 75% of the FC in the first year and 85% of the FC in the 2nd year. In fact, in two growing seasons, the rainfall amount from March 1 to April

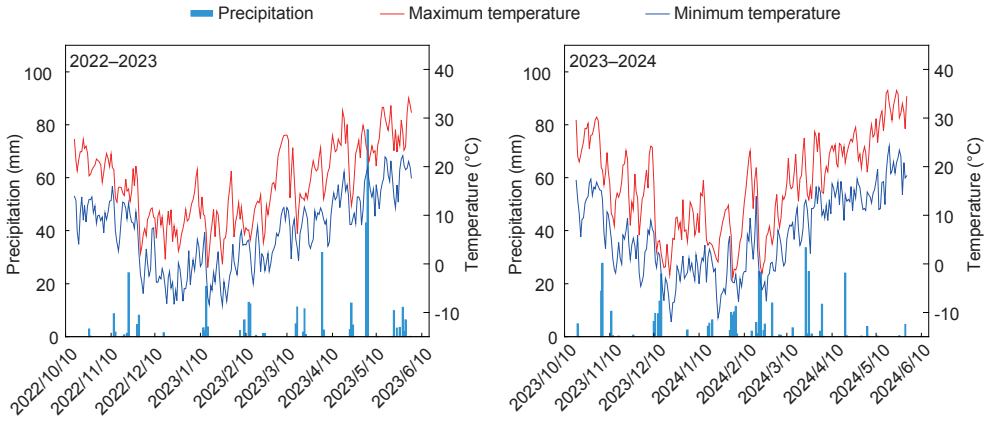


Fig. 1 Daily precipitation and weather temperature in the two growing seasons of winter wheat.

30 is 103.6 and 83.0 mm, respectively. In the 2022–2023 growing season, wheat entered the jointing (Z31), booting (Z45), and anthesis (Z61) stages on March 13, April 14, and April 22, respectively, with soil water falling below the irrigation threshold at all stages, and supplemental irrigation amounts were 7.80, 9.65, and 24.89 mm, totaling 42.34 mm. In 2023–2024, the respective stages occurred on March 8, April 7, and April 18. Soil water dropped below the threshold during the jointing (Z31) and booting (Z45) stages, requiring irrigation of 32.16 and 29.10 mm, totaling 61.26 mm. The sum of rainfall and irrigation volume from March 1 to April 30 is 145.9 and 144.3 mm during the two growing seasons of wheat. The calculation method for micro-sprinkler irrigation volume is adopted as specified (Guo *et al.* 2015). Although soil water exceeded 85% FC at the anthesis stage, 5 mm of irrigation was applied to assist fertilization, resulting in a total irrigation amount of 66.26 mm. The experimental plots, which measured 4 m by 40 m (160 m^2) each, had three repetitions for each treatment. The wheat seeds were sown manually, and the row spacing for sowing was 20 cm, with 20 rows per plot. The micro-sprinkler tapes were laid between the 5th and 6th rows and between the 15th and 16th rows. Phosphorus (P_2O_5) and potassium (K_2O) fertilizers were applied at rates of 112.5 kg ha^{-1} before sowing. Total nitrogen application was 202.5 kg ha^{-1}, with 112.5 kg ha^{-1} as the base fertilizer for the CI and MI, and all the nitrogen was applied as base fertilizer for RI. For MI, urea (46.5% N) was used as topdressing, fully dissolved in the fertilization system at the jointing (Z31), booting (Z45), and anthesis (Z61) stages, with each time providing 30 N kg ha^{-1}, while 90 N kg ha^{-1} was spread over the fields for CI before irrigation at the jointing stage. The irrigation regimes and nitrogen fertilization quantities for the different treatments are shown in Table 1. The sowing dates for the two seasons were October 21, 2022, and October 18, 2023. The planting density after emergence was approximately 225 plants m^{-2}. The harvest (Z91) dates were June 3, 2023 and May 30, 2024, respectively.

2.3. Sampling and measurement

Soil water content (SWC) To measure water content, soil was sampled at 20 cm intervals from the 1 m depth in each experimental plot before wheat sowing, as well as at the jointing, booting, anthesis, and maturity stages. After weighing the samples, they were placed in an oven to dry to constant weight to measure the SWC (Li J P *et al.* 2025).

Biochemical assays in flag leaf 200 spikes that reached anthesis on the same day were chosen and labeled in each plot. On the 4 days after anthesis (DAA 4, the grain-developing stage) and the DAA 20 (the grain-filling stage), 10 labeled main stem flag leaves were randomly sampled from each treatment with three repetitions. The samples were immediately frozen in liquid nitrogen and then stored in a –80°C freezer for later analysis.

(1) Chlorophyll content

The chlorophyll content was determined using the alcohol extraction method (Li *et al.* 2018). The samples were finely chopped under low temperature, 0.10 g of leaf tissue was weighed, and 25 mL of 95% ethanol was added. The samples were then incubated at room temperature in the dark for 48 h, with occasional shaking. The absorbance of the extract was measured at wavelengths of 665 and 649 nm using a UV spectrophotometer. The chlorophyll content was calculated using the following formula:

$$\text{Chlorophyll content}=\frac{(13.95A_{665}-6.88A_{649})V}{W}+\frac{(24.96A_{649}-7.32A_{665})V}{W} \quad (1)$$

where A is the absorbance of the extract, V is the volume of the extraction solution, and W is the leaf weight.

(2) Rubisco and sucrose phosphate synthase (SPS) activities

The activities of SPS in the flag leaf were measured using the enzyme-linked immunosorbent assay (ELISA) (Yang *et al.* 2001), with ELISA kits provided by Shanghai Meilian Bio Co., Ltd., China.

Sucrose and soluble sugar content Main stems with consistent flowering time and uniform growth were selected on DAA 4 and 20, and 10 plants were sampled for each treatment. The plants were decomposed into flag leaves, grains, and the remaining parts. The plants were weighed after being dried to a consistent weight at 75°C. Soluble sugar content was determined using the anthrone colorimetric method (Jia and Zhang 2008), and sucrose content was determined using the resorcinol colorimetric method (Winter and Huber 2000).

Grain endosperm cell number Some main stem spikes were randomly selected from each treatment on DAA 10 and 20, and four grains were sampled from the same position on each spike. The samples were fixed with FAA, and endosperm cell peeling, staining, separation, filtration, observation, and counting were performed as described by Gong *et al.* (2019). The number of endosperm cells per unit

Table 1 Irrigation regimes and nitrogen fertilization quantities for three treatments

Year	Treatment[1)]	Irrigation stage and amount (mm)[2)]				N application stage and amount (kg ha^{-1})[2)]				
		JS	BS	AS	Total	SS	JS	BS	AS	Total
2022–2023	RI	0	0	0	0	202.5	0	0	0	202.5
	CI	60	0	0	60	112.5	90	0	0	202.5
	MI	7.80	9.65	24.89	42.34	112.5	30	30	30	202.5
2023–2024	RI	0	0	0	0	202.5	0	0	0	202.5
	CI	60	0	0	60	112.5	90	0	0	202.5
	MI	32.16	29.10	5.00	66.26	112.5	30	30	30	202.5

[1)] RI, rain-fed; CI, conventional flood irrigation; MI, micro-sprinkler irrigation.
[2)] SS, before seed sowing; JS, jointing stage; BS, booting stage; AS, anthesis stage.

area (2.5×10^5 μm^2) was observed under the microscope.

Grain hormone content and starch synthase activity A total of 10 labeled main stem spikes were randomly selected from each treatment on DAA 4 and 20 and sampled from all the grains in the middle part of the spikes (4 to 12 spikelets). The contents of ZR, indole propionic acid (IPA), GA, IAA, and ABA hormones, as well as the activities of adenosine diphosphate glucose pyrophosphorylase (AGPase), soluble starch synthase (SSS), granule-bound starch synthase (GBSS), and starch branching enzyme (SBE), were determined using ELISA kits provided by Shanghai Meilian Bio Co., Ltd. (Yang *et al.* 2001).

Grain starch content A total of 10 labeled main stem spikes were randomly selected from each treatment at the grain filling (DAA 20) and maturity stages and sampled from all the grains in the middle part of the spikes. The samples were dried at 75°C until a constant weight was achieved. Starch content was determined using the dual-wavelength method (Hansen and Møller 1975).

Grain-filling parameters Fifty wheat spikes that flowered on the same day on plants with similar overall plant height, ear height, and stem diameter were selected and tagged for each experimental plot. Ten tagged ears from each plot were sampled at 7-day intervals from the tenth day after anthesis to maturity. The samples were dried at 75°C to constant weight, then weighed, and the filling rate was calculated. The grain-filling process was fitted with logistic equations as follows (Lv *et al.* 2017):

$$Y=\frac{K}{(1+Ae^{-Bt})} \quad (2)$$

where Y is the theoretical 1,000-grain weight (TGW) (g), K is the theoretical maximum TGW (g), t is the time after anthesis (d), and A and B are the coefficients determined by regression. The filling phase was calculated from the derivative of the equation. The end of the early, middle, and late grain-filling stages was defined as t_1=(lnB–1.317)/C, t_2=(lnB+1.317)/C, and t_3=(lnB+4.59512)/C, respectively. After dry weight determination, the dried grains were reserved for analyzing nitrogen concentrations and calculating grain protein concentration during the filling period.

Grain yield and yield components Prior to harvest, 2 m^2 of each plot was randomly chosen throughout the harvest season to determine the spike number, and 50 spikes were randomly selected to measure the number of grains per spike. The grain yield of winter wheat was measured by weighing the grain from a 2 m^2 area after maturity in each experimental area and expressed as 13% of grain water content. From each sample, 1,000 grains were randomly selected and weighed to measure the TGW.

2.4. Statistical analysis

The two-way analysis of variance (two-way ANOVA) in SPSS software version 26.0 (SPSS Inc., Chicago, IL, USA) was used to analyze the effects of different irrigation methods and years on various parameters of winter wheat. Mean comparisons were performed using the least significant difference (LSD) method at a significance level of 0.05. Figures and tables were created using Origin 2024 software (OriginLab Corp., Northampton, MA, USA).

3. Result

3.1. Variation in SWC

In both growing seasons, soil water content (SWC) showed distinct variations among irrigation treatments and across different soil depths (Fig. 2). Under RI, SWC was generally low and decreased steadily throughout the growth stages, with the 0–40 cm soil layer frequently suffering from water deficits. Compared with RI, CI increased soil water from jointing to anthesis; however, its soil water distribution across growth stages and soil depths varied considerably, lacking stability and persistence. In contrast, MI maintained higher SWC in the 0–40 cm layer across all growth stages compared to RI and CI treatments. Over the two years, MI significantly increased (P<0.05) SWC in the 0–60 cm layer at the anthesis stage and the grain-filling period relative to CI.

3.2. Flag leaf chlorophyll content

The chlorophyll content in the flag leaf of wheat decreased from DAA 4 to 20, with significant differences among different irrigation treatments (Fig. 3). Both the year type (Y) and irrigation mode (I) had a highly significant (P<0.01) effect on the chlorophyll content of the flag leaf in both DAA 4 and 20, with no significant (P>0.05) interactive effect between Y and I. At DAA 4 and 20, the chlorophyll content in MI was significantly higher (P<0.05) than CI, and CI was significantly higher (P<0.05) than RI. In 2022–2023, the chlorophyll content in RI, CI, and MI decreased by 20.54, 18.14, and 14.18%, respectively, from DAA 4 to 20. The decrease in MI was 30.96 and 21.84% less than in RI and CI, respectively. In 2023–2024, the chlorophyll content in RI, CI, and MI decreased by 34.79, 30.17, and 27.56%, respectively. The decrease in MI was 20.80 and 8.68% less than in RI and CI, respectively.

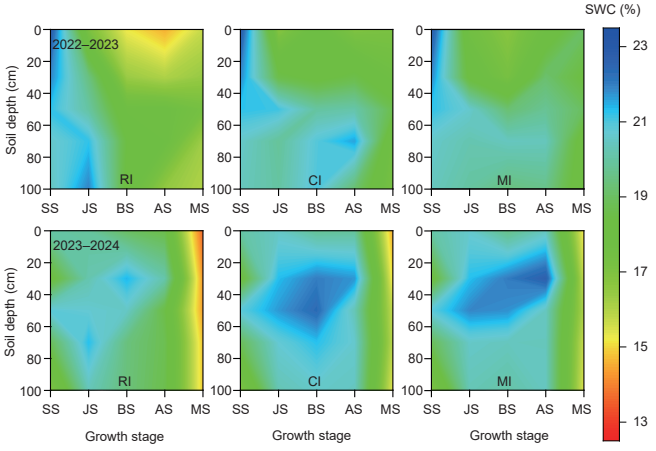


Fig. 2 Effects of different irrigation treatments on the soil water content (SWC) of the 1-m soil profile in the two growing seasons of winter wheat. SS, before seed sowing; JS, jointing stage; BS, booting stage; AS, anthesis stage; MS, maturity stage. RI, rain-fed; CI, conventional flood irrigation; MI, micro-sprinkler irrigation.

3.3. Flag leaf Rubisco activity

Rubisco activity in the flag leaf of wheat decreased from DAA 4 to 20, with significant differences among different irrigation treatments (Fig. 4). Both the year type and irrigation mode had a highly significant (P<0.01) effect on the Rubisco activity of the flag leaf in both DAA 4 and 20, with no significant (P>0.05) interactive effect between the two factors. At DAA 4 in 2022–2023, Rubisco activity in RI was significantly lower (P<0.05) than in CI and MI, with no significant difference (P>0.05) between MI and CI. At DAA 20, MI was significantly higher (P<0.05) than CI, and CI was significantly higher (P<0.05) than RI. Compared to RI and CI, the decrease in MI was reduced by 62.43 and 65.46% from DAA 4 to 20, respectively. In 2023–2024, MI was significantly higher (P<0.05) than CI, and CI was significantly higher (P<0.05) than RI at DAA 4, while the trend at DAA 20 was consistent with that of 2022–2023. Compared to RI and CI, the decrease in MI was reduced by 40.31 and 26.87% from DAA 4 to 20, respectively.

3.4. Flag leaf SPS activity

The SPS activity in the flag leaf of wheat decreased from DAA 4 to 20, with significant differences among different irrigation treatments (Fig. 5). Both the year type and irrigation mode had a highly significant (P<0.01) effect on the SPS activity of the flag leaf in both DAA 4 and 20, with no significant (P>0.05) interactive effect between Y and I. In 2022–2023, the SPS activity in RI was significantly lower (P<0.05) than in CI and MI at DAA 4, with no significant (P>0.05) difference between MI and CI. At DAA 20, MI was significantly higher (P<0.05) than CI, and CI was significantly higher (P<0.05) than RI. Compared to RI and CI, the decrease in MI was reduced by 49.03 and 34.57% from DAA 4 to 20, respectively. In 2023–2024, MI was significantly higher (P<0.05) than CI, and CI was significantly higher (P<0.05) than RI at DAA 4, while the trend at DAA 20 was consistent with that of 2022–2023. Compared to RI and CI, the decrease in MI was reduced by 48.77 and 30.45% from DAA 4 to 20, respectively.

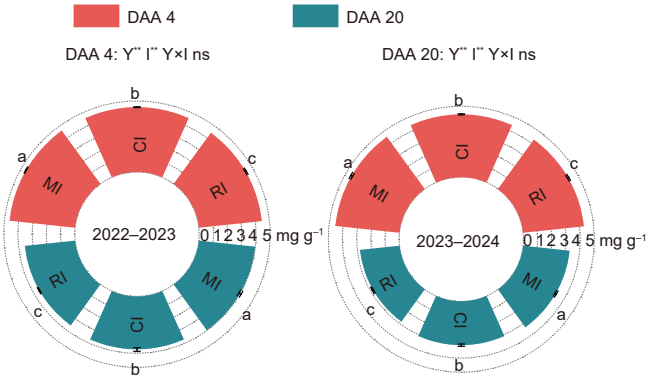


Fig. 3 Effects of different irrigation treatments on the chlorophyll content of the flag leaf after anthesis in the two growing seasons of winter wheat. RI, rain-fed; CI, conventional flood irrigation; MI, micro-sprinkler irrigation. DAA, days after anthesis. Bars represent standard errors (n=3). Different letters stand for significant differences at P<0.05. ** indicates significance at P<0.01; ns indicates no significance.

3.5. Sucrose and soluble sugar content in flag leaf and grain

As shown in Table 2, both the year type and irrigation mode had a significant effect (P<0.01) on the soluble sugar and sucrose contents in the flag leaf and grains at DAA 4 and 20. Moreover, the soluble sugar and sucrose contents in the flag leaf at DAA 20 were affected by the interactive effect of Y and I (P<0.01). Meanwhile, the soluble sugar content in grain at DAA 4 (P<0.05), as well as the sucrose content (P<0.01) and soluble sugar content (P<0.01) in grain at DAA 20, were all significantly influenced by the interactive effect of Y and I. In 2022–2024, the sucrose and soluble sugar content in grain from DAA 4 to 20 were consistently higher in MI than in CI, and higher in CI than in RI. In 2022–2023, the sucrose and soluble sugar content in the flag leaf were significantly lower (P<0.05) in RI than in CI and MI at DAA 4, with no significant difference (P>0.05) between CI and MI. At DAA 20, the sucrose and soluble sugar content in the flag leaf were

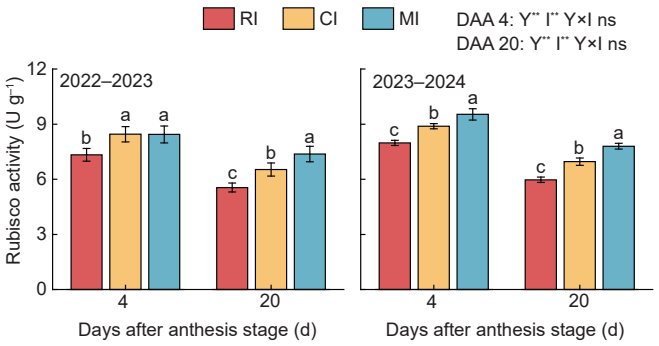


Fig. 4 Effects of different irrigation treatments on the enzyme activity of Rubisco in the flag leaf after anthesis in the two growing seasons of winter wheat. RI, rain-fed; CI, conventional flood irrigation; MI, micro-sprinkler irrigation. Bars represent standard errors (n=3). Different letters stand for significant differences at P<0.05. ** indicates significance at P<0.01; ns indicates no significance.

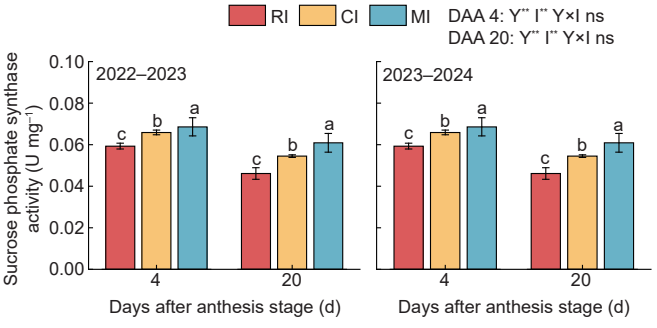


Fig. 5 Effects of different irrigation treatments on the enzyme activity of sucrose phosphate synthase activity (SPS) in the flag leaf after anthesis in the two growing seasons of winter wheat. RI, rain-fed; CI, conventional flood irrigation; MI, micro-sprinkler irrigation. DAA, days after anthesis. Bars represent standard errors (n=3). Different letters stand for significant differences at P<0.05. ** indicates significance at P<0.01; ns indicates no significance.

significantly higher (P<0.05) in MI than in CI, and higher in CI than in RI. In 2023–2024, the sucrose and soluble sugar content in the flag leaf were consistently higher in MI than in CI, and higher in CI than in RI from DAA 4 to 20.

3.6. Grain endosperm cell number

As shown in Fig. 6, both year type and irrigation mode had a significant effect (P<0.01) on grain endosperm cell number at DAA 10 and 20, with no significant interactive effect (P>0.05) between Y and I. In 2022–2023, the number of endosperm cells per unit area in the grain was significantly higher (P<0.05) in MI than in CI and RI at DAA 10, with RI showing the lowest number. Compared to RI and CI, MI increased by 26.83 and 14.29%, respectively. At DAA 20, the trends were consistent with those observed at DAA 10, with MI showing increases in endosperm cell number of 14.81 and 7.83% compared to RI and CI, respectively. In 2023–2024, the results followed the same pattern as in 2022–2023. At DAA 10, MI increased by 42.17 and 20.24% compared to RI and CI, respectively. At DAA 20, MI showed increases of 75.21 and 33.12% compared to RI and CI, respectively.

3.7. Grain endogenous hormone content

As shown in Fig. 7, whether at DAA 4 or 20, the irrigation mode had a significant effect on the contents of different hormones (P<0.01). Except for IPA+ZR at DAA 4, as well as GA and ABA at DAA20, the year type exerted a significant effect on these hormone contents (P<0.05 or P<0.01). Only IPA+ZR and ABA at DAA 4 were significantly affected (P<0.05) by the interactive effect of Y and I. In 2022–2023, the IPA+ZR content was significantly lower (P<0.05) in RI than in CI and MI at DAA 4, and MI was significantly higher (P<0.05) than RI at DAA 20. The level of IAA in RI was significantly higher (P<0.05) than CI and MI at DAA 4, and MI was significantly higher (P<0.05) than CI, with RI showing the lowest levels at DAA 20. The GA content in MI was significantly higher (P<0.05) than in RI at DAA 4, and the trend at DAA 20 was consistent with the IPA+ZR. The ABA content in RI was significantly higher (P<0.05) than in CI and MI at DAA 4, while RI was significantly higher (P<0.05) than CI, and MI showed the lowest levels at DAA 20. In 2023–2024, the IPA+ZR and GA content in MI were significantly higher (P<0.05) than in CI, and CI was higher than RI at DAA 4, while the IAA and ABA levels in RI were significantly higher (P<0.05) than in CI, and MI showed the lowest levels. At DAA 20, the IAA, IPA+ZR, and GA content in MI was significantly higher (P<0.05) than in CI, and CI was significantly higher (P<0.05) than RI, while ABA was the lowest in MI, with CI significantly lower (P<0.05) than RI.

Table 2 Effects of different irrigation treatments on sucrose and soluble sugar content in the flag leaf and grain after anthesis in the two growing seasons of winter wheat

Year	Organ	Treatment[1)]	4 days after anthesis		20 days after anthesis	
			Sucrose content (mg g^{-1})	Soluble sugar content (mg g^{-1})	Sucrose content (mg g^{-1})	Soluble sugar content (mg g^{-1})
2022–2023	Flag leaf	RI	36.75 b	46.16 b	23.38 c	29.94 c
		CI	40.63 a	51.36 a	25.57 b	32.88 b
		MI	43.16 a	53.31 a	27.23 a	34.91 a
	Grain	RI	52.88 c	81.42 c	17.82 c	27.18 c
		CI	57.14 b	88.56 b	19.21 b	29.69 b
		MI	60.61 a	95.31 a	20.73 a	31.67 a
2023–2024	Flag leaf	RI	43.67 c	52.10 c	31.82 c	35.87 c
		CI	47.85 b	58.11 b	36.78 b	41.75 b
		MI	51.29 a	61.10 a	41.34 a	47.37 a
	Grain	RI	56.76 c	87.12 c	21.30 c	36.49 c
		CI	63.23 b	101.73 b	25.00 b	43.04 b
		MI	67.75 a	116.88 a	27.42 a	45.79 a
ANOVA	Flag leaf	Year (Y)	**	**	**	**
		Irrigation (I)	**	**	**	**
		Y×I	ns	ns	**	**
	Grain	Y	**	**	**	**
		I	**	**	**	**
		Y×I	ns	*	**	**

[1)] RI, rain-fed; CI, conventional flood irrigation; MI, micro-sprinkler irrigation.
Values followed by different letters within a column of the same organ in each year stand for significant differences at P<0.05. * and ** indicate significances at P<0.05 and P<0.01, respectively; ns indicates no significance.

3.8. Grain starch synthesis

Both year type and irrigation mode had significant effects (P<0.01) on the activities of SSS, GBSS, SBE, and AGPase (Table 3). Except for AGPase activity, the other indicators were significantly affected (P<0.01) by the interactive effect of Y×I. In 2022–2023, the SSS activity in MI was significantly higher (P<0.05) than in CI and RI, with no significant difference (P>0.05) between CI and RI. In 2023–2024, SSS activity in MI was significantly higher (P<0.05) than in CI, and CI was significantly higher (P<0.05) than RI. In 2022–2024, the activities of GBSS, SBE, and AGPase in MI were all significantly higher (P<0.05) than in CI and RI, with RI showing the lowest activity.

According to Table 4, the contents of amylose, amylopectin, and total starch at the filling and maturity stages were significantly affected by Y (P<0.01) and I (P<0.01), and the

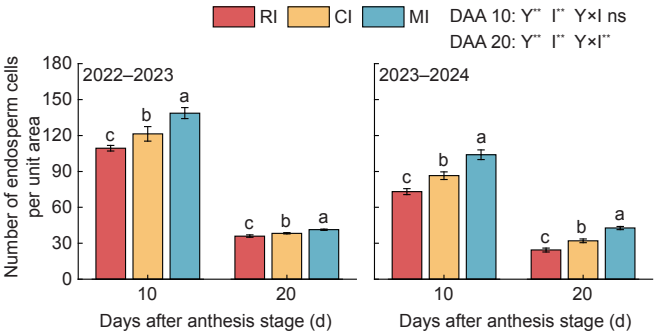


Fig. 6 Effects of different irrigation treatments on the number of endosperm cells per unit area after anthesis in the two growing seasons of winter wheat. RI, rain-fed; CI, conventional flood irrigation; MI, micro-sprinkler irrigation. DAA, days after anthesis. Bars represent standard errors (n=3). Different letters stand for significant difference at P<0.05. ** indicate significances at P<0.01; ns indicates no significance.

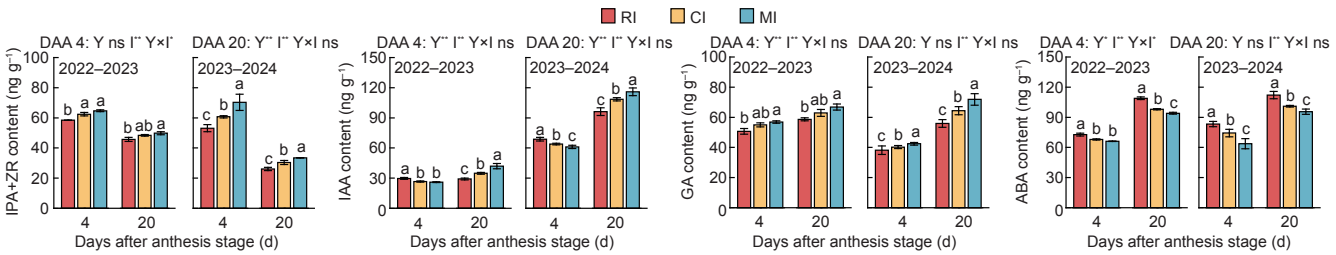


Fig. 7 Effects of different irrigation treatments on the contents of endogenous hormones in grain after anthesis during the two growing seasons of winter wheat. RI, rain-fed; CI, conventional flood irrigation; MI, micro-sprinkler irrigation. IPA, indole propionic acid; ZR, zeatin nucleoside; IAA, auxin; GA, gibberellin; ABA, abscisic acid. DAA, days after anthesis. Bars represent standard errors (n=3). Different letters stand for significant differences at P<0.05. * and ** indicate significances at P<0.05 and P<0.01, respectively; ns indicates no significance.

Table 3 Effects of different irrigation treatments on starch synthesis key enzymes activity of grain at the grain-filling stage in the two growing seasons of winter wheat[1)]

Year	Treatment[1)]	SSS activity (U g^{-1})	GBSS activity (U g^{-1})	SBE activity (U g^{-1})	AGPase activity (U mg^{-1})
2022–2023	RI	9.11 b	1.93 c	3.60 c	4.42 c
	CI	9.38 b	2.49 b	3.78 b	4.96 b
	MI	10.07 a	2.74 a	4.07 a	5.82 a
2023–2024	RI	12.31 c	2.52 c	5.97 c	7.58 c
	CI	14.18 b	2.83 b	6.23 b	8.09 b
	MI	15.70 a	3.05 a	6.88 a	8.60 a
ANOVA					
Year (Y)		**	**	**	**
Irrigation (I)		**	**	**	**
Y×I		**	**	**	ns

[1)] SSS, soluble starch synthase; GBSS, granule-bound starch synthase; SBE, starch branching enzyme; AGPase, adenosine diphosphate glucose pyrophosphorylase.
[2)] RI, rain-fed; CI, conventional flood irrigation; MI, micro-sprinkler irrigation.
Values followed by different letters within a column in each year stand for significant differences at P<0.05. ** indicates significance at P<0.01; ns indicates no significance.

amylose content was also significantly affected (P<0.01) by Y×I. The contents of amylose, amylopectin, and total starch in grain in MI were significantly higher (P<0.05) than in CI, and CI was significantly higher (P<0.05) than RI at the grain filling and maturity stages. The amylose content in MI increased by 8.10 and 2.66%, respectively, compared to RI and CI in 2022–2023, and by 17.87 and 10.14% in 2023–2024 at the grain-filling stage. Compared to RI and CI, the amylopectin content in MI increased by 12.55 and 5.50% in 2022–2023, and by 10.37 and 6.00% in 2023–2024, respectively.

3.9. Dynamics of grain weight formation

According to Fig. 8, except for DAA10, both the year type and irrigation mode had a significant effect (P<0.01) on the TGW and grain-filling rate at all other stages. Additionally, Y and I exhibited a significant interactive effect (P<0.05) on the TGW at DAA 17, and a significant effect (P<0.01) on the grain-filling rate at DAA 17, DAA 24 (P<0.01), and DAA 38 (P<0.05). Across the two years, grain-filling rates at different stages were consistent with grain weight, with MI showing the highest rates and CI higher than RI. As grain weight continued to increase, the difference between treatments was most apparent at DAA 38. In 2022–2023, the grain weight in MI was 9.96 and 3.26% higher than in RI and CI, and it was 9.18 and 4.90% higher in 2023–2024, respectively. The grain-filling rate peaked at DAA 24 in both years. In 2022–2023, the peak rate for MI was 6.46 and 2.56% higher than for CI and RI, respectively; in 2023–2024, it was 15.04 and 8.62% higher, respectively. The peak for MI also occurred later than for CI and RI.

3.10. Grain-filling parameters

As shown in Table 5, except for t1, all other indicators were highly significantly affected by Y (P<0.01) and I (P<0.01). Additionally, W0 (P<0.05), Tm (P<0.01), t1 (P<0.01), t2 (P<0.01), and t3 (P<0.05) were influenced by the interactive effect of Y and I. In both years of the experiment, MI significantly increased (P<0.05) the theoretical maximum grain weight (W0) and maximum filling rate (Vm). Compared to RI, W0 and Vm in MI increased by 11.81 and 10.00%, respectively, in 2022–2023, and by 9.46 and 3.49%, respectively, in 2023–2024. MI also significantly delayed (P<0.05) the time to reach the maximum filling rate (Tm), extended the total filling duration, and increased the filling rate, particularly during the acceleration phase (v1). In 2022–2023 and 2023–2024, v1 in MI was 10.96 and 6.25% higher than in RI, respectively.

3.11. Grain yield and yield components

As shown in Table 6, the effects of year type and irrigation mode on winter wheat grain yield were significant (P<0.001), while the interaction between Y and I also had a significant effect (P<0.01) on grain yield. In 2022–2023, the grain yield in MI was significantly higher (P<0.05) than in RI and CI, increasing by 15.60 and 4.99%, respectively; in 2023–2024, it increased by 39.14 and 11.60%, respectively. In both years, irrigation treatments significantly affected yield components (P<0.001). MI significantly increased (P<0.05) the number of spikes, number of grains per spike, and TGW of wheat. Specifically, the TGW in MI was 7.33 and 4.99% higher than in RI and CI in 2022–2023, and 11.51 and 5.55% higher in 2023–2024, respectively.

3.12. Correlation analysis among different traits

As shown in Fig. 9, in this study, by analyzing the correlation between indicators, we found that there was a significantly positive correlation (P<0.05 or P<0.01) between grain weight, Rubisco activity, SPS activity, the contents of sucrose and soluble sugar (SS), and the IPA+ZR content of DAA 4. However, grain weight showed a significantly negative correlation (P<0.05) with ABA content in grain under DAA 4. At DAA 20, the activities of Rubisco and SPS in the flag leaf, the contents of sucrose and SS in the flag leaf, and the contents of IAA and GA in grain showed a significantly positive correlation (P<0.01) between grain weight, while the ABA content in grain was significantly negative correlation (P<0.01) with grain weight.

4. Discussion

4.1. Effects of different irrigation regimes on flag leaf physiology of wheat after anthesis

The source–sink relationship refers to the dynamic balance between the biosynthesis capacity of photosynthetic organs (source) and the uptake and assimilation of these substances by grains (sink). Within this framework, the photosynthate supply capacity of the source and the resource absorption efficiency of the sink synergistically regulate the efficiency of material translocation, partitioning, and conversion in crops, which plays a pivotal role in grain yield formation (Fang *et al.* 2024; Wang *et al.* 2024). As the primary organ of wheat for photosynthesis after anthesis, the flag leaf serves as its most critical “source”, and its photosynthetic capacity exerts a

Table 4 Effects of different irrigation treatments on starch content of grain in the two growing seasons of winter wheat

Year	Treatment[1)]	Amylose content (%)		Amylopectin content (%)		Total starch content (%)	
		Filling stage	Maturity stage	Filling stage	Maturity stage	Filling stage	Maturity stage
2022–2023	RI	5.95 c	16.63 c	22.58 c	13.33 c	50.89 c	64.22 c
	CI	6.26 b	17.74 b	24.00 b	14.28 b	52.10 b	66.38 b
	MI	6.43 a	18.72 a	25.15 a	15.10 a	52.96 a	68.06 a
2023–2024	RI	6.64 c	18.15 c	24.80 c	15.09 c	52.13 c	67.21 c
	CI	7.11 b	18.90 b	26.01 b	16.24 b	53.63 b	69.97 b
	MI	7.83 a	20.04 a	27.87 a	17.22 a	54.98 a	72.21 a
ANOVA							
Year (Y)		**	**	**	**	**	**
Irrigation (I)		**	**	**	**	**	**
Y×I		**	ns	ns	ns	ns	ns

[1)] RI, rain-fed; CI, conventional flood irrigation; MI, micro-sprinkler irrigation.
Values followed by different letters within a column in each year stand for significant differences at P<0.05. ** indicates significance at P<0.01; ns indicates no significance.

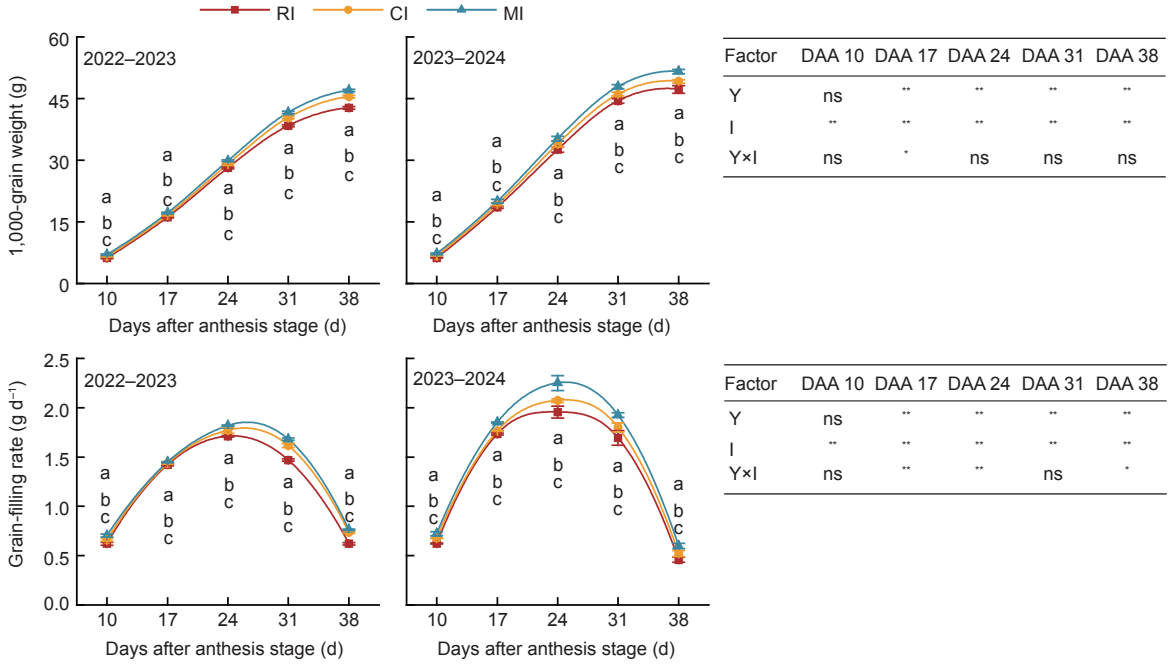


Fig. 8 Effects of different irrigation treatments on the grain weight accumulation and grain-filling rate after anthesis during the two growing seasons of winter wheat. RI, rain-fed; CI, conventional flood irrigation; MI, micro-sprinkler irrigation. The blue, brown, and red lowercase letters represent MI, CI, and RI, respectively. DAA, days after anthesis. Y, year; I, irrigation. Different letters stand for significant differences at P<0.05. Bars represent standard errors (n=3). * and ** indicate significances at P<0.05 and P<0.01, respectively; ns indicates no significance.

Table 5 Effect of different irrigation treatments on the grain filling parameters in the two growing seasons of winter wheat[1)]

Year	Treatment[2)]	W0 (mg)	Vm (mg d^{-1})	Tm (d)	t1 (d)	t2 (d)	t3 (d)	v1 (mg d^{-1})	v2 (mg d^{-1})	v3 (mg d^{-1})
2022–2023	RI	45.30 c	1.80 c	20.82 b	12.51 b	29.14 c	48.69 c	0.73 c	1.62 c	0.45 b
	CI	48.83 b	1.94 b	21.39 a	12.77 a	30.02 b	50.32 b	0.77 b	1.68 b	0.46 a
	MI	50.65 a	1.98 a	21.48 a	12.71 a	30.24 a	50.85 a	0.81 a	1.72 a	0.47 a
2023–2024	RI	49.36 c	2.29 b	19.90 c	12.53 c	27.28 c	44.62 c	0.80 b	1.99 c	0.55 b
	CI	51.25 b	2.34 a	20.18 b	12.67 b	27.69 b	45.34 b	0.82 a	2.02 b	0.56 a
	MI	54.03 a	2.37 a	20.72 a	12.92 a	28.52 a	46.86 a	0.85 a	2.06 a	0.57 a
ANOVA										
Year (Y)		**	**	**	ns	**	**	**	**	**
Irrigation (I)		**	**	**	**	**	**	**	**	**
Y×I		*	ns	**	**	**	*	ns	ns	ns

[1)] W0, Vm, and Tm delegate the theoretical 1,000-grain weight, maximum filling rate, and time to maximum filling rate, respectively. t1, t2, and t3 represent the ending time of the lag, mid, and late stages, respectively. v1, v2, and v3 delegate the grain-filling rate of the lag, mid, and late stages, respectively.
[2)] RI, rain-fed; CI, conventional flood irrigation; MI, micro-sprinkler irrigation.
Values followed by different letters within a column of the same organ in each year stand for significant differences at $P<0.05$; * and ** indicate significances at $P<0.05$ and $P<0.01$, respectively; ns indicates no significance.

Table 6 Effects of different irrigation treatments on yield and its components in the two growing seasons of winter wheat

Year	Treatment[1)]	Spike number (×10^4 ha^{-1})	Grain number per spike	1,000-grain weight (g)	Grain yield (kg ha^{-1})
2022–2023	RI	571.95 c	39.59 c	43.49 c	9,344.67 c
	CI	631.98 b	41.09 b	44.46 b	10,288.48 b
	MI	720.36 a	43.29 a	46.68 a	10,802.07 a
2023–2024	RI	533.58 c	29.75 c	44.40 c	6,934.37 c
	CI	593.75 b	34.56 b	46.90 b	8,645.79 b
	MI	660.00 a	39.96 a	49.51 a	9,648.52 a
ANOVA					
Year (Y)		**	***	***	***
Irrigation (I)		***	***	***	***
Y×I		ns	**	*	**

[1)] RI, rain-fed; CI, conventional flood irrigation; MI, micro-sprinkler irrigation. Y, year; I, irrigation.
Values followed by different letters within a column in each year stand for significant differences at $P<0.05$. *, ** and *** indicate significances at $P<0.05$, $P<0.01$ and $P<0.001$, respectively; ns indicates no significance.

decisive effect on assimilate supply. In this study, compared with RI and CI, MI significantly increased chlorophyll content, Rubisco activity, and SPS activity in wheat flag leaf during the ovary-developing stage (DAA 4) (Fig. 3). Consequently, the contents of sucrose and soluble sugar in MI were significantly elevated (Table 2), which provided adequate carbohydrate to support endosperm cell proliferation and expand the "sink" capacity (Fig. 6). During the grain-filling stage (DAA 20), MI significantly delayed flag leaf senescence, maintained photosynthetic capacity, and slowed the decline in chlorophyll content and enzyme activity compared with RI and CI (Figs. 3–5). This indicates that under RI conditions, wheat may face water stress during the later growth stage, leading to leaf chlorophyll degradation and a decline in photosynthetic enzyme activity (Pang *et al.* 2024). In this study, the results also confirmed that under RI, the SWC was the lowest during the anthesis and grain-filling stages of wheat, and MI was significantly higher than CI (Fig. 2). This indicates that compared with other treatments, MI can better meet the water demand during the grain formation and filling stages, thereby enhancing the assimilate supply capacity and promoting the improvement of sink capacity. Furthermore, soil nitrogen availability is likely to be higher under MI, which in turn exerts a certain promotional effect on strengthening source function and facilitating grain formation. Collectively, these effects effectively alleviate the water and nitrogen deficit that wheat may encounter after anthesis, maintain an appropriate metabolic environment and normal physiological functions in leaves, and thus ensure the sustained "source" activity of wheat and the continuous supply of nutrients during the grain formation period (Zhang *et al.* 2023; Ma *et al.* 2024; Zhao *et al.* 2024).

4.2. Effects of different irrigation regimes on grain-filling dynamics of winter wheat

Grain soluble sugar and starch accumulation directly determines grain quality and weight, and reflects the efficiency of source–sink transport and utilization. During the grain-filling stage, starch synthase in the grain plays a key role in converting sugars into starch (Luo *et al.* 2019). In this study, compared with RI and CI, MI significantly increased sugar accumulation in grain (Table 2) by enhancing sink capacity (Fig. 6) and promoting grain assimilation of photosynthates. It also accelerated sugar-to-starch conversion by increasing starch synthase activity (Table 3), thus promoting starch accumulation in grain (Table 4).

Grain weight is a critical indicator of wheat yield, and its changes are regulated by soil water and nitrogen supply after anthesis (Yao *et al.* 2024). Studies have shown that grain-filling rate and duration are decisive factors affecting grain weight (Wu *et al.* 2022). When wheat encounters drought stress during grain filling, it can accelerate cell aging, prematurely terminate the filling process, and cause insufficient accumulation of filling materials, ultimately leading to reduced grain plumpness (Abdelrahman *et al.* 2020). In this study, compared with RI, both CI and MI significantly increased grain weight and filling rate during the grain-filling stage, and MI exhibited the best performance (Fig. 8). Logistic equation fitting of the filling process showed that MI significantly increased the maximum filling rate and delayed the time to reaching the maximum filling rate,

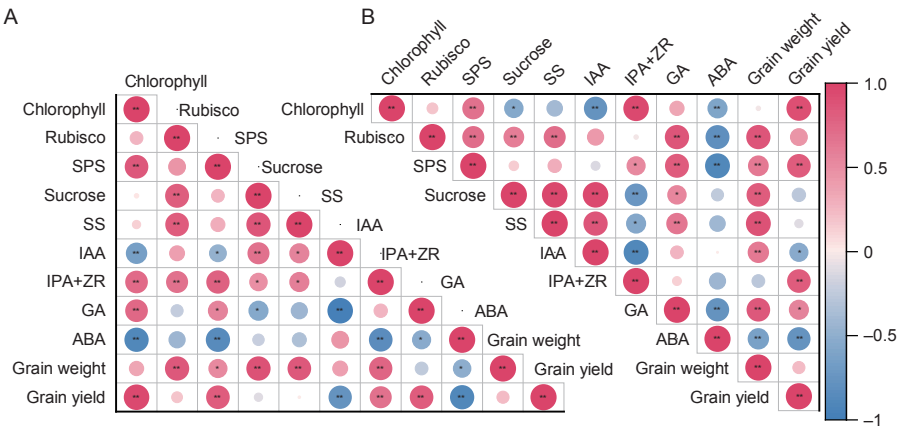


Fig. 9 Relationships between different parameters and grain weight in this study. Different colors indicate the intensity of the significance, and the closer to red (positive) or blue (negative), the higher the significance. A represents 4 days after anthesis (DAA 4); B represents DAA 20. SPS, sucrose phosphate synthase; SS, soluble sugar; IAA, auxin; IPA, indole propionic acid; ZR, zeatin nucleoside; GA, gibberellin; ABA, abscisic acid. * and ** indicate significances at $P<0.05$ and $P<0.01$, respectively.

thereby increasing the theoretical maximum grain weight (Table 5). This suggests that under MI, grains exhibit higher yield potential and a faster filling rate, and this irrigation method maintains a more stable and continuous grain-filling process. Although CI also increased grain weight compared with RI through top-dressing and supplemental irrigation, it failed to maintain the stability and continuity of the filling process. While some studies have found a stronger correlation between grain weight and the filling duration (Dias and Lidon 2009), others suggest that grain weight is mainly influenced by the maximum filling rate (Huang *et al.* 2003). This may be because the filling rate is primarily controlled by genetic factors, while filling duration is mainly influenced by environmental factors (Huang *et al.* 2003). Existing studies have reported inconsistent conclusions, which can be ascribed to variations in wheat variety, cultivation measures, climatic conditions, and other confounding factors. Consistently, discrepancies were observed in the parameter fitting results between the two experimental years of the present study. Compared with 2022–2023, the maximum filling rate in 2023–2024 was higher, the filling duration was shorter, but the final grain weight increased. This may suggest that, under the conditions of the HP, the grain weight of this wheat variety is more closely linked to the maximum filling rate. Besides, the jointing to booting stage of wheat is also a critical period for the development of young spikes and florets. A reasonable supply of water and nitrogen during this stage is crucial for increasing spike number and grain number per spike (Li J P *et al.* 2025). In this study, we found that, compared with CI, MI not only increased wheat grain weight but also enhanced the number of grains per spike and the number of spikes per unit area (Table 6). This finding differs from previous studies (Li *et al.* 2021; Yao *et al.* 2023), which may be attributed to the precise control of water supply and topdressing nitrogen fertilizer. These factors promote root growth, enhance leaf nutrient absorption, improve water and nitrogen use efficiency, and ultimately increase the number of spikes and grains per spike. However, under RI and CI, they may reduce the availability of soil water and nitrogen during the booting period, failing to meet the requirements for spike and floret development, thereby leading to decreases in SN and KN. Future studies could investigate the mechanisms by which micro-sprinkler irrigation promotes wheat tillering and spike differentiation, providing scientific evidence to optimize irrigation management for wheat production in the HP region.

4.3. Effects of different irrigation regimes on hormonal metabolism during grain development

Wheat grain development results from endosperm cell proliferation and filling, with the cell size influenced by early-stage endosperm cell division and subsequent filling. These processes are regulated by endogenous hormones. Research has shown that optimizing water and nitrogen management to regulate hormone balance can improve drought tolerance and yield potential in cereal crops (Cao *et al.* 2018; Zhao *et al.* 2023). Different hormones participate in regulating cell growth and assimilate synthesis and transport, thereby influencing grain development (Yang *et al.* 2006). ZR+IPA, as one of the key endogenous hormones, primarily increases the number of endosperm cells by promoting cell division, enhancing the “sink potential” of the grain, and providing a structural foundation for nutrient accumulation (Lv *et al.* 2017). IAA, a promotive hormone, plays various roles at different stages of endosperm development. In this study, during the grain formation stage (DAA 4), the ZR+IPA content was significantly higher under MI compared to RI, while the IAA content was lower than in RI (Fig. 7). This may be attributed to the fact that a high IAA level signals a transition from endosperm cell division to expansion. Research has shown a positive correlation between IAA and starch content (Forestan *et al.* 2010), with IAA promoting starch synthesis by regulating AGPase subunits and glucose-6-phosphate isomerase expression to complete grain filling (Lur and Setter 1993; McAdam *et al.* 2017). The results suggest that MI increased IAA content

during the early-stage (DAA 4) and promoted cytokinin synthesis, encouraging continuous cell division and delaying the transition to the volume growth phase, thus increasing in endosperm cell number (Fig. 6). At DAA 20, the ZR+IPA content began to decline, while IAA content increased, signaling the end of endosperm cell proliferation and the shift to the grain filling. At this point, MI significantly increased IAA content, consistent with the changes in starch synthase activity (Table 3), further confirming the role of IAA in regulating starch synthesis. ABA also plays a critical regulatory role in grain development, primarily by promoting leaf senescence and inhibiting cell division to facilitate grain development completion (Lei *et al.* 2022). In this study, compared with RI, MI significantly reduced ABA content in grain and delayed its rapid accumulation at DAA 20, which in turn effectively extended the grain-filling duration and provided more time for grain development. Additionally, the reduction in ABA content might have weakened its antagonistic effect on GA and IAA, allowing IAA and ZR+IPA to act longer during grain filling (Yang and Zhang 2006). Some studies suggest that while GA regulates wheat grain filling, it may not be the decisive factor in the process (Ali *et al.* 2018). In this study, MI significantly increased GA content during grain filling (Fig. 7), which may have enhanced endosperm cell activity, promoting the transport of more photosynthetic products to the grain (Binenbaum *et al.* 2018; Vishal and Kumar 2018). In conclusion, the grain-filling process is not regulated by a single hormone but by the interaction of multiple hormones. Therefore, optimizing the dynamic balance between hormones is key to improving wheat grain weight. Future research should focus on elucidating how antagonistic and synergistic hormonal interactions in grain regulate the expression of synthesis genes and signal transduction pathways, thereby further clarifying their regulatory mechanisms during wheat grain filling.

5. Conclusion

Micro-sprinkler irrigation (MI) significantly optimized the source–sink relationship in wheat, resulting in a notable increase in grain weight and yield in the HP region. Compared with conventional flood irrigation (CI) and rain-fed (RI) conditions, MI significantly delayed flag leaf senescence, increased chlorophyll content after anthesis, and enhanced photosynthetic enzyme activity, thereby improving photosynthetic capacity during the grain-filling stage and promoting the accumulation and transport of photosynthetic products. Additionally, MI significantly enhanced the activity of sucrose-phosphate synthase (SPS) in the flag leaf and increased the contents of sucrose and soluble sugar in both the flag leaf and grain compared with CI and RI treatments, providing sufficient carbohydrate substrates for grain filling. MI also significantly promoted endosperm cell proliferation, increased the grain-filling rate, extended the filling duration, accelerated the conversion of carbohydrates into starch, and increased starch content. In terms of hormonal regulation, MI significantly increased the contents of IAA, ZR+IPA, and GA in grain during the filling stage while reducing ABA content. This extended the grain-filling duration, optimized the dynamic hormonal balance, and ultimately facilitated grain development and grain weight formation.

Acknowledgements

We sincerely appreciate the funding from the National Key Research and Development Program of China (2023YFD2301505), the Talent Introduction Project of Anhui Agricultural University, China (yj2019-01), and the Planting Project of Modern Industrial Technology System of the “14th Five-year Plan” of Anhui Province, China (340000222426000100009).

Declaration of competing interest

The authors declare that they have no conflict of interest.

Declaration of generative AI and AI-assisted technologies in the writing process

During the preparation of this manuscript, the authors used ChatGPT 4.0 to assist in improving the clarity and readability of the language. All content generated was carefully reviewed and revised by the authors as necessary, and the authors take full responsibility for the final content of the article.

References

Abdelrahman M, Burritt D J, Gupta A, Tsujimoto H, Tran L S P. 2020. Heat stress effects on source–sink relationships and metabolome dynamics in wheat. *Journal of Experimental Botany*, **71**, 543–554.

Ahmed M, Bilal M, Ahmad S. 2024. Simulation of source sink partitioning in wheat under varying nitrogen regimes using DSSAT-CERES-wheat model. *Agricultural Water Management*, **303**, 109028.

Ali S, Xu Y Y, Ahmad I, Jia Q M, Huang F Y, Daur I, Wei T, Cai T, Ren X L, Zhang P, Jia Z K. 2018. The ridge furrow cropping technique indirectly improves seed filling endogenous hormonal changes and winter wheat production under simulated rainfall conditions. *Agricultural Water Management*, **204**, 138–148.

Alonso M P, Abbate P E, Mirabella N E, Aramburu Merlos F, Panelo J S, Pontaroli A C. 2018. Analysis of sink/source relations in bread wheat recombinant inbred lines and commercial cultivars under a high yield potential environment. *European Journal of Agronomy*, **93**, 82–87.

Bao X Y, Zhang B Y, Dai M L, Liu X J, Ren J H, Gu L M, Zhen W C. 2024. Improvement of grain weight and crop water productivity in winter wheat by light and frequent irrigation based on crop evapotranspiration. *Agricultural Water Management*, **301**, 108922.

Binenbaum J, Weinstain R, Shani E. 2018. Gibberellin localization and transport in plants. *Trends in Plant Science*, **23**, 410–421.

Cao X C, Zhu C Q, Zhong C, Hussain S, Zhu L F, Wu L H, Jin Q Y. 2018. Mixed-nitrogen nutrition-mediated enhancement of drought tolerance of rice seedlings associated with photosynthesis, hormone balance and carbohydrate partitioning. *Plant Growth Regulation*, **84**, 451–465.

Che Z Q, Bie S T, Wang R R, Ma Y L, Zhang Y Y, He F F, Jiang G Y. 2025. Mild deficit irrigation delays flag leaf senescence and increases yield in drip-irrigated spring wheat by regulating endogenous hormones. *Journal of Integrative Agriculture*, **24**, 2954–2973.

Dias A S, Lidon F C. 2009. Evaluation of grain filling rate and duration in bread and durum wheat, under heat stress after anthesis. *Journal of Agronomy and Crop Science*, **195**, 137–147.

Fan Y H, Qin B Y, Yang J H, Ma L L, Cui G J, He W, Tang Y, Zhang W J, Ma S Y, Ma C X, Huang Z L. 2024. Night warming increases wheat yield by improving pre-anthesis plant growth and post-anthesis grain starch biosynthesis. *Journal of Integrative Agriculture*, **23**, 536–550.

Fang H, Liu F L, Gu X B, Chen P P, Li Y P, Li Y N. 2022. The effect of source-sink on yield and water use of winter wheat under ridge-furrow with film mulching and nitrogen fertilization. *Agricultural*

Water Management, **267**, 107616.
Fang L, Struik P C, Girousse C, Yin X Y, Martre P. 2024. Source–sink relationships during grain filling in wheat in response to various temperature, water deficit, and nitrogen deficit regimes. *Journal of Experimental Botany*, **75**, 6563–6578.
Farooq M, Wahid A, Kobayashi N, Fujita D, Basra S M A. 2009. Plant drought stress: Effects, mechanisms and management. *Agronomy*, **29**, 185–212.
Feng S W, Gu S B, Zhang H B, Wang D. 2017. Root vertical distribution is important to improve water use efficiency and grain yield of wheat. *Field Crops Research*, **214**, 131–141.
Forestan C, Meda S, Varotto S. 2010. *ZmPIN1*-mediated auxin transport is related to cellular differentiation during maize embryogenesis and endosperm development. *Plant Physiology*, **152**, 1373–1390.
Furbank R T, Sharwood R, Estavillo G M, Silva-Perez V, Condon A G. 2020. Photons to food: Genetic improvement of cereal crop photosynthesis. *Journal of Experimental Botany*, **71**, 2226–2238.
Gong Y, Guo Y Y, Wang G Y, Chen Z P, Duan W W. 2019. Effect of nitrogenous topdressing period on endosperm proliferation and grain filling characteristics of winter wheat. *Journal of Triticeae Crops*, **39**, 427–477. (in Chinese)
Gou Q Q, Zhu Y H, Horton R, Lv H S, Wang Z L, Su J B, Cui C Y, Zhang H Q, Wang X Y, Zheng J Y, Yuan F. 2020. Effect of climate change on the contribution of groundwater to the root zone of winter wheat in the Huaibei Plain of China. *Agricultural Water Management*, **240**, 106292.
Guo Z J, Shi Y, Yu Z W, Zhang Y L. 2015. Supplemental irrigation affected flag leaves senescence post-anthesis and grain yield of winter wheat in the Huang-Huai-Hai Plain of China. *Field Crops Research*, **180**, 100–109.
Hansen J, Møller I. 1975. Percolation of starch and soluble carbohydrates from plant tissue for quantitative determination with anthrone. *Analytical Biochemistry*, **68**, 87–94.
Hao B Z, Ma J L, Si S H, Wang X J, Wang S L, Li F M, Jiang L N. 2024. Response of grain yield and water productivity to plant density in drought-tolerant maize cultivar under irrigated and rainfed conditions. *Agricultural Water Management*, **298**, 108880.
Hisse I R, D'Andrea KE, Otegui M E. 2019. Source-sink relations and kernel weight in maize inbred lines and hybrids: Responses to contrasting nitrogen supply levels. *Field Crops Research*, **230**, 151–159.
Huang X Q, Cöster H, Ganal M W, Röder M S. 2003. Advanced backcross QTL analysis for the identification of quantitative trait loci alleles from wild relatives of wheat (*Triticum aestivum* L.). *Theoretical and Applied Genetics*, **106**, 1379–1389.
Jia W S, Zhang J H. 2008. Stomatal movements and long-distance signaling in plants. *Plant Signaling & Behavior*, **3**, 772–777.
Lei L, Wu D, Cui C, Gao X, Yao Y J, Dong J, Xu L S, Yang M M. 2022. Transcriptome analysis of early senescence in the post-anthesis flag leaf of wheat (*Triticum aestivum* L.). *Plants*, **11**, 2593.
Li J P, Wang S Q, Li Z W, Xing K Y, Tao X F, Wang Z M, Zhang Y H, Yao C S, Li J C. 2025. Effects of micro-sprinkler irrigation and topsoil compaction on winter wheat grain yield and water use efficiency in the Huaibei Plain, China. *Journal of Integrative Agriculture*, **24**, 2974–2988.
Li J P, Wang Y Q, Zhang M, Liu Y, Xu X X, Lin G, Wang Z M, Yang Y H, Zhang Y H. 2019. Optimized micro-sprinkling irrigation scheduling improves grain yield by increasing the uptake and utilization of water and nitrogen during grain filling in winter wheat. *Agricultural Water Management*, **211**, 59–69.
Li J P, Wang Z M, Yao C S, Zhang Z, Liu Y, Zhang Y H. 2021. Micro-sprinkling irrigation simultaneously improves grain yield and protein concentration of winter wheat in the North China Plain. *Crop Journal*, **9**, 1397–1407.
Li J P, Xu X X, Lin G, Wang Y Q, Liu Y, Zhang M, Zhou J Y, Wang Z M, Zhang Y H. 2018. Micro-irrigation improves grain yield and resource use efficiency by co-locating the roots and N-fertilizer distribution of winter wheat in the North China Plain. *Science of the Total Environment*, **643**, 367–377.
Li Z W, Liu H L, Wang K K, Yao C S, Wang Z M, Zhang Y H, Li J C, Song Y H, Li J P. 2025. Micro-sprinkling irrigation and topsoil compaction improve seedling quality of winter wheat in the Huaibei Plain of China. *Plant and Soil*, **507**, 967–984.
Liu Y, Liang H Y, Lv X K, Liu D D, Wen X X, Liao Y C. 2016. Effect of polyamines on the grain filling of wheat under drought stress. *Plant Physiology and Biochemistry*, **100**, 113–129.
Lu X L, Yu Z W, Zhang Y L, Shi Y. 2019. Study on water consumption characteristics and dry matter assimilation accumulation and distribution of different spike type wheat varieties under supplemental irrigation based on soil moisture. *Journal of Triticeae Crops*, **39**, 1489–1493. (in Chinese)
Luo J, Wei B, Han J, Liao Y C, Liu Y. 2019. Spermidine increases the sucrose content in inferior grain of wheat and thereby promotes its grain filling. *Frontiers in Plant Science*, **10**, 1309.
Lur H S, Setter T L. 1993. Role of auxin in maize endosperm development (timing of nuclear DNA endoreduplication, zein expression, and cytokinin). *Plant Physiology*, **103**, 273–280.
Lv X K, Han J, Liao Y C, Liu Y. 2017. Effect of phosphorus and potassium foliage application post-anthesis on grain filling and hormonal changes of wheat. *Field Crops Research*, **214**, 83–93.
Lv X M, Zhang Y, Zhang Y X, Fan S J, Kong L G. 2020. Source-sink modifications affect leaf senescence and grain mass in wheat as revealed by proteomic analysis. *BMC Plant Biology*, **20**, 257.
Ma B, Zhang L, He Z H. 2023. Understanding the regulation of cereal grain filling: The way forward. *Journal of Integrative Plant Biology*, **65**, 526–547.
Ma Y L, Wang H Q, Liu J G, Wang R R, Che Z Q. 2024. Effects of root trace nitrogen reduction in arid areas on sucrose-starch metabolism of flag leaves and grains and yield of drip-irrigated spring wheat. *Agronomy*, **14**, 312.
Maydup M L, Antonietta M, Guiamet J J, Graciano C, López J R, Tambussi E A. 2010. The contribution of ear photosynthesis to grain filling in bread wheat (*Triticum aestivum* L.). *Field Crops Research*, **119**, 48–58.
McAdam E L, Meitzel T, Quittenden L J, Davidson S E, Dalmais M, Bendahmane A I, Thompson R, Smith J J, Nichols D S, Urquhart S, Gélinas-Marion A, Aubert G, Ross J J. 2017. Evidence that auxin is required for normal seed size and starch synthesis in pea. *New Phytologist*, **216**, 193–204.
Morris R O, Blevins D G, Dietrich J T, Durley R C, Gelvin S B, Gray J, Hommes N G, Kaminek M, Mathews L J, Meilan R, Reinbott T M, Sayavedra-Soto L. 1993. Cytokinins in plant pathogenic bacteria and developing cereal grains. *Functional Plant Biology*, **20**, 621.
Pang H F, Lian Y H, Zhao Z B, Guo H, Li Z Z, Hu J J, Ren Y Z, Lin T B, Wang Z Q. 2024. Compensatory effect of supplementary irrigation on winter wheat under warming conditions. *Agricultural Water Management*, **295**, 108778.
Peleg Z, Reguera M. Tumimbang E, Walia H, Blumwald E. 2011. Cytokinin-mediatedsource/sink modifications improve drought tolerance and increase grain yield in rice underwater-stress. *Plant Biotechnology Journal*, **9**, 747–758.
Ru C, Hu X T, Wang W E, Yan H. 2024. Impact of nitrogen on photosynthesis, remobilization, yield, and efficiency in winter wheat under heat and drought stress. *Agricultural Water Management*, **302**, 109013.
Sehgal A, Sita K, Siddique K H M, Kumar R, Bhogireddy S, Varshney R K, HanumanthaRao B, Nair R M, Prasad P V V, Nayyar H. 2018. Drought or/and heat-stress effects on seed filling in food crops: Impacts on functional biochemistry, seed yields, and nutritional quality. *Frontiers in Plant Science*, **9**, 1705.
Serrago R A, Alzueta I, Savin R, Slafer G A. 2013. Understanding grain yield responses to source-sink ratios during grain filling in wheat and barley under contrasting environments. *Field Crops Research*, **150**, 42–51.
Thapa S, Jessup K E, Pradhan G P, Rudd J C, Liu S, Mahan J R, Devkota R N, Baker J A, Xue Q W. 2018. Canopy temperature depression at grain filling correlates to winter wheat yield in the U.S. Southern High Plains. *Field Crops Research*, **217**, 11–19.
Vishal B, Kumar P P. 2018. Regulation of seed germination and abiotic stresses by gibberellins and abscisic acid. *Frontiers in Plant Science*, **9**, 838.
Wang D. 2017. Water use efficiency and optimal supplemental irrigation in a high yield wheat field. *Field Crops Research*, **213**, 213–220.
Wang H G, Yu Z W, Shi Y, Zhang Y L. 2020. Effects of tillage practices on grain yield formation of wheat and the physiological mechanism in rainfed areas. *Soil & Tillage Research*, **202**, 104675.
Wang R R, Kong L T, Bie S T, Tu H M, Cai J Y, Jiang G Y, Xu J W. 2024. Agronomic evaluation of wheat (*Triticum aestivum* L.) under

different degrees of drought-rehydration conditions under drip irrigation. *Agronomy*, **14**, 2968.
Wang Z Q, Xu Y J, Chen T T, Zhang H, Yang J C, Zhang J H. 2015. Abscisic acid and the key enzymes and genes in sucrose-to-starch conversion in rice spikelets in response to soil drying during grain filling. *Planta*, **241**, 1091–1107.
Winter H, Huber S C. 2000. Regulation of sucrose netabolism in higher plants: Localization and regulation of activity of key enzymes. *Critical Reviews in Plant Sciences*, **19**, 31–67.
Wu X L, Miao L L, Li C S, Allen D M, Li M, Xiong T, Liu Y B, Tang T L. 2022. Source–sink relations and responses to sink–source manipulations during grain filling in wheat. *Journal of Integrative Agriculture*, **21**, 1593–1605.
Xia H Y, Wang L, Qiao Y T, Kong W L, Xue Y H, Wang Z S, Kong L.G, Xue Y F, Sizmur T. 2020. Elucidating the source–sink relationships of zinc biofortification in wheat grains: A review. *Food and Energy Security*, **9**, e243.
Xie Q, Mayes S, Sparkes D L. 2015. Carpel size, grain filling, and morphology determine individual grain weight in wheat. *Journal of Experimental Botany*, **66**, 6715–6730.
Xu Z Z, Yu Z W, Wang D. 2006. Nitrogen translocation in wheat plants under soil water deficit. *Plant and Soil*, **280**, 291–303.
Yan S C, Wu Y, Fan J L, Zhang F C, Qiang S C, Zheng J, Xiang Y Z, Guo J J, Zou H Y. 2019. Effects of water and fertilizer management on grain filling characteristics, grain weight and productivity of drip-fertigated winter wheat. *Agricultural Water Management*, **213**, 983–995.
Yang J C, Zhang J H. 2006. Grain filling of cereals under soil drying. *New Phytologist*, **169**, 223–236.
Yang J C, Zhang J H, Liu K, Wang Z Q, Liu L J. 2006. Abscisic acid and ethylene interact in wheat grains in response to soil drying during grain filling. *New Phytologist*, **171**, 293–303.
Yang J C, Zhang J H, Wang Z Q, Zhu Q S, Wang W. 2001. Hormonal changes in the grains of rice subjected to water stress during grain filling. *Plant Physiology*, **127**, 315–323.
Yang X Y, Asseng S, Wong M T F, Yu Q, Li J, Liu E. 2013. Quantifying the interactive impacts of global dimming and warming on wheat yield and water use in China. *Agricultural and Forest Meteorology*, **182–183**, 342–351.
Yao C S, Li J P, Gao Y M, Zhang Z, Liu Y, Sun Z C, Wang Z M, Zhang Y H. 2024. Delayed application of water and fertilizer increased wheat yield but did not improve quality parameters. *Field Crops Research*, **319**, 109649.
Yao C S, Li J P, Zhang Z, Liu Y, Wang Z M, Sun Z C, Zhang Y H. 2023. Improving wheat yield, quality and resource utilization efficiency through nitrogen management based on micro-sprinkler irrigation. *Agricultural Water Management*, **282**, 108277.
Yu H X, Duan X X, Sun A Q, Sun X X, Zhang J J, Sun H Q, Sun Y Y, Ning T Y, Tian J C, Wang D X, Li H, Fan K X, Wang A P, Ma W J, Chen J S. 2022. Genetic dissection of the grain-filling rate and related traits through linkage analysis and genome-wide association study in bread wheat. *Journal of Integrative Agriculture*, **21**, 2805–2817.
Zadoks J C, Chang T T, Konzak C F. 1974. A decimal code for the growth stages of cereals. *Weed Research*, **14**, 415–421.
Zhai L C, Lv L H, Dong Z Q, Zhang L H, Zhang J T, Jia X L, Zhang Z B. 2021. The water-saving potential of using micro-sprinkling irrigation for winter wheat production on the North China Plain. *Journal of Integrative Agriculture*, **20**, 1687–1700.
Zhang Y, Qiang S C, Zhang G X, Sun M, Wen X X, Liao Y C, Gao Z Q. 2023. Effects of ridge-furrow supplementary irrigation on water use efficiency and grain yield of winter wheat in Loess Plateau of China. *Agricultural Water Management*, **289**, 108537.
Zhang Z, Li J, Zheng X Y, Li J P, Liu Y, Sun W, Ren J, Xiao X C, Zhang W Q, Sun Z C, Wang Z M, Zhang Y H. 2024. Ovary morphology determines ovary-to-grain transition process and final grain weight potential in wheat. *European Journal of Agronomy*, **159**, 127233.
Zhang Z, Yu Z W, Zhang Y L, Shi Y. 2021. Finding the fertilization optimization to balance grain yield and soil greenhouse emissions under water-saving irrigation. *Soil & Tillage Research*, **214**, 105167.
Zhao J K, Xu X X, Liu S, Jia J, Li M L, Huang H L, Zhang G Q, Zhao C X. 2024. Optimizing wheat prosperity: Innovative drip irrigation and nitrogen management strategies for enhanced yield and quality of winter wheat in the Huang-Huai-Hai region. *Frontiers in Plant Science*, **15**, 1454205.
Zhao L, Tang Q Y, Song Z W, Yin Y G, Wang G D, Li Y X. 2023. Increasing the yield of drip-irrigated rice by improving photosynthetic performance and enhancing nitrogen metabolism through optimizing water and nitrogen management. *Frontiers in Plant Science*, **14**, 1075625.

Executive Editor-in-Chief Shaokun Li
Managing Editor Ning Wang